Redistribution of nerve strain enables end-to-end repair under tension without inhibiting nerve regeneration

Holly M. Howarth[1, #], Turki Alaziz[2, #], Brogan Nicolds[1], Shawn O'Connor[3], Sameer B. Shah[1, 2, 4, *]

1 Department of Bioengineering, University of California, San Diego, La Jolla, CA, USA
2 Department of Orthopaedic Surgery, University of California, San Diego, La Jolla, CA, USA
3 School of Exercise and Nutritional Sciences, San Diego State University, San Diego, CA, USA
4 Research Service, VA San Diego Healthcare System, San Diego, CA, USA

Abstract
End-to-end repair under no or low tension leads to improved outcomes for transected nerves with short gaps, compared to repairs with a graft. However, grafts are typically used to enable a tension-free repair for moderate to large gaps, as excessive tension can cause repairs to fail and catastrophically impede recovery. In this study, we tested the hypothesis that unloading the repair interface by redistributing tension away from the site of repair is a safe and feasible strategy for end-to-end repair of larger nerve gaps. Further, we tested the hypothesis that such an approach does not adversely affect structural and functional regeneration. In this study, we used a rat sciatic nerve injury model to compare the integrity of repair and several regenerative outcomes following end-to-end repairs of nerve gaps of increasing size. In addition, we proposed the use of a novel implantable device to safely repair end-to-end repair of larger nerve gaps by redistributing tension away from the repair interface. Our data suggest that redistriubution of tension away from the site of repair enables safe end-to-end repair of larger gap sizes. In addition, structural and functional measures of regeneration were equal or enhanced in nerves repaired under tension – with or without a tension redistribution device – compared to tension-free repairs. Provided that repair integrity is maintained, end-to-end repairs under tension should be considered as a reasonable surgical strategy. All animal experiments were performed under the approval of the Institutional Animal Care and Use Committee of University of California, San Diego (Protocol S11274).

*Correspondence to:
Sameer B. Shah, PhD,
sbshah@ucsd.edu,

 # These two authors contributed equally to this work.

orcid:
0000-0001-6613-3904
(Sameer B. Shah)

Introduction

Peripheral nerve injuries can be devastating to an individual's sensorimotor capabilities and quality of life. Though nerves are capable of regeneration, structural and functional recovery is hindered by the fact that growth tends to be highly disorganized (Meek et al., 2005). For complete nerve transections, functional recovery is especially poor, as axons must successfully and accurately regrow from the proximal stump into and through the distal stump, and reconnect at motor or sensory termini. As positive outcomes are not typically observed for weeks to months following surgery, surgical decision-making at the time of repair is of the utmost importance (Pfister et al., 2011).

End-to-end repair is preferred for transected nerves with short gaps (Meek et al., 2005; Bhatia et al., 2017). However, if such a repair places the nerve or the site of repair under substantial tension, outcomes are likely to be poor and repair failure emerges as a significant concern (Terzis et al., 1975; Maeda et al., 1999; Sunderland et al., 2004); so, an intervening graft or conduit is deployed. Hollow conduits are acceptable for relatively short gaps, but for modest to long gaps, autografts remain the gold-standard (Matsuyama et al., 2000; Siemionow and Sonmez, 2010; Grinsell and Keating, 2014). Despite their utility, autografts have many disadvantages, including additional patient exposure to anesthesia, donor site morbidity, geometry mismatches between injured and donor nerves, and the presence of multiple interfaces across which axons must grow before even reaching the distal nerve (Schmidt and Leach, 2003). On the other hand, despite the prevalence of graft-based repairs, there is increasing evidence that low to moderate tension may be beneficial to nerve regeneration. *In vivo* and *ex vivo* models suggest accelerated axonal or nerve outgrowth under tension (Bray, 1984; Pfister et al., 2004; Franz and Guck, 2010; Simpson et al., 2014), and direct end-to-end nerve repairs under slight tension in fact outperform tension-free graft repairs for modest nerve gaps (Hentz et al., 1993; Sunderland et al., 2004).

In this study, we tested the hypothesis that redistributing tension away from the site of repair will enable the end-to-end repair of larger nerve gaps. Further, we hypothesize that such a strategy will not adversely affect structural and functional regeneration. In this study, we compare the integrity of repair and several regenerative outcomes in end-to-end repairs of varying nerve gaps (*i.e.*, varying tension). In addition, we propose the use of a novel implantable device to safely repair end-to-end repair of larger nerve gaps by redistributing tension away from the repair interface.

Materials and Methods

Nerve-interfacing device
A nerve-interfacing device (NID; patent pending) was designed to redistribute tension away from the repair site (**Figure 1**). The device consists of two hemi-cylindrical clamps – one for each stump – which grip the nerve. A stainless steel guide rod connects the two clamps, and allows alignment and approximation of nerve ends to a desired strain during

or after repair. Several additional design features enable the nerve to be secured without excessive compression: i) Epineurial barbs oriented against the direction of tension, to secure the nerve during repair and subsequent loading; ii) overlying sutures, to ensure that the nerve does not slip; iii) a hemicylindrical interface with the nerve, with a diameter slightly larger than that of the nerve, to ensure that the nerve is not excessively compressed by the sutures; iv) small footprint, to enable device to be seated within the nerve bed without modifying the nerve trajectory (*i.e.*, no appreciable raising of the nerve from its bed); v) clamp biocompatibility and customization; clamps were printed on a Projet 3510 HD 3D Printer (3D Systems, Rock Hill, SC, USA) using Visijet M3 Crystal (USP class VI approved).

Nerve transection and repair
All animal experiments were performed under the approval of the Institutional Animal Care and Use Committee of University of California, San Diego (Protocol S11274). Surgeries were performed on 10–12 week old male (250–300 g; *n* = 38) Lewis rats (Envigo, Placentia, CA, USA) by an orthopedic surgeon after multiple successful practice repairs in terminal procedures that were inspected for quality by a senior attending hand surgeon. Anesthesia was induced with 5% isoflurane/95% oxygen, and maintained at 2% isoflurane/98% oxygen for the duration of the surgery. For survival surgery, anesthetized rats were injected with 0.03 mg/mL buprenorphine (Par Pharmaceutical, Chestnut Ridge, NY, USA) and Baytril (Bayer Healthcare, Shawnee Mission, KS, USA). Sciatic nerves of the right hindlimb were exposed by splitting the femoral biceps, and decompressed prior to transection and repair.

Two cohorts were tested. The first cohort (terminal surgery, *n* = 16) was divided into four groups. In the first three groups, 0, 2, or 3 mm of nerve (corresponding to no, moderate, or high tension) were removed following transection, to test the integrity of end-to-end repair during hindlimb joint manipulation in a terminal surgery (**Figure 1A**). In the 4th group, a 3 mm gap was created, and an NID deployed to redistribute tension away from the repair site. The nerve was placed within the clamp and sutured using 4-0 Nurolon (Ethicon, Guaynabo, Puerto Rico) to the device (**Figure 1B**). Clamps were brought together along the guide rod such that the repair site was tension free, and strain was redistributed proximally and distally. The proximal cuff was secured to underlying muscle with a single 4-0 suture, such that any device movement did not tether or excessively load the intact proximal stump. Nerves were repaired end-to-end with three epineurial stitches (8-0 Ethilon suture, Ethicon), with the knee and ankle in a neutral configuration. After this initial repair, maximum physiological strain was imposed on the nerve: with hips abducted, knees were fully extended (180 degrees) and ankles maximally dorsi-flexed. This loading was repeated three times. Typically, repair failure occurred immediately; however, joints were held in position for 2 minutes to allow for the possibility of slower failure. The integrity of repairs was then visually assessed using digital

images, and additional epineurial sutures used to reinforce failed or failing repairs.

The second cohort (survival surgery, *n* = 18) was subdivided into three groups (**Figure 1A–D**). In group 1 (0 mm gap), the nerve was transected without any additional gap. In groups 2 (3 mm) and 3 (3 mm-NID), a 3 mm length of nerve was removed following transection. Nerves in all groups were repaired end-to-end with exactly three stitches around the nerve circumference. In group 3, the NID was implanted following repair as above (**Figure 1E** and **1F**). Contralateral nerves were decompressed, and served as sham controls. After surgery, in all groups, overlying muscle was sutured using 4-0 polyglycolide suture (Oasis, Mettawa, IL, USA), then skin was stapled together using AutoClips (MikRon Precision, Gardena, CA, USA). Rats were allowed to recover on a heating pad before being returned to their cages. Buprenorphine was provided twice a day for 3 days, for analgesia.

After 12 weeks, rats were anesthetized and the sciatic nerve was exposed as in the first surgery. Devices were removed, sciatic nerves from both legs were harvested, pinned to cork, frozen in liquid nitrogen cooled isopentane, and stored at –80°C until processing.

Biomechanical testing
During survival surgery (second cohort), 10-0 Ethilon (Ethicon) sutures were stitched into the epineurium, two proximal and two distal to the injury site, as markers to measure proximal and distal strain, respectively, using methods previously published (Mahan et al., 2015). Suture spacing was measured in two configurations – tension-free (1, knee and ankle neutral) and nerve tensioned (2, full knee extension and neutral ankle; ankles were not dorsiflexed to avoid damage observed in terminal studies (first cohort) with maximum physiological nerve strain). The length between the sutures was recorded before the injury (L_{pre1}, L_{pre2}), immediately after the injury and repair (L_{post1}, L_{post2}), and at 12 weeks just before tissue harvest ($L_{recovery1}$, $L_{recovery2}$). Strain was measured before injury ($L_{pre2}-L_{pre1}$)/L_{pre2}, immediately after injury and repair ($L_{post2}-L_{post1}$)/L_{post2}, and twelve weeks after repair (*i.e.*, just before sacrifice) proximal and distal to the injury site ($L_{recovery2}-L_{recovery1}$)/$L_{recovery2}$, based on the change in marker spacing with nerves under tension compared to untensioned. In addition, as an indirect measure of growth, the spacing between markers in a tension free configuration was compared at 12 weeks after recovery *vs.* just after repair ($L_{recovery1}-L_{post1}$)/L_{post1}, the rationale being that an increase in spacing reflects material addition between the sutures.

Electromyography testing
To test the effect of clamping on nerve conduction in an uninjured nerve (*i.e.*, to test whether the device interface has the potential to damage the nerve by compression), sciatic nerves were exposed during a terminal surgery in a third cohort (*n* = 10). After decompression, clamps were secured onto intact nerves, as above. Nerve conduction velocity was assessed using previously published methods (Restaino et al., 2014; Love et al., 2017), 10–15 minutes following device

implantation. Briefly, nerves were stimulated with a miniature bipolar hook electrode (Item ID: 501650; Harvard Apparatus, Holliston, MA, USA) positioned at either of two locations proximal to the clamp, separated by 5 mm. Two monopolar needle recording electrodes (Grass F-E2) were positioned adjacent to the endplate zone (Westerga and Gramsbergen, 1993), and a ground needle electrode was placed in the contralateral limb. Stimulation pulses (SD9, Grass Instruments, Astro-Med Inc., West Warwick, RI, USA) were chosen to minimize the applied voltage, while maintaining a recordable and consistent electromyography response (6 monophasic 50 μs duration square pulses at 5 Hz, at an input voltage of 7 V (< 10 mA)). Five recordings were made at each location to ensure consistency of stimulation and recording, and averaged together to determine the latency between stimulus and recording. Velocity was measured based on the 5 mm spacing divided by the difference in latency between the recorded signals for each stimulation location.

Functional testing
To test hindlimb function, rats were run and recorded on a Treadscan treadmill (CleverSys Inc., Reston, VA, USA) for 20 seconds at a rate of 10 cm/s, given a brief period to rest, then run a second time. Data points were collected pre-operatively, then at 2 and 12 weeks post-operatively. The sciatic functional index (SFI) was measured by two lab members, one blinded to experimental groups. Video stills were taken at points in time where the rat fully placed its paw on the track during normal gait. The length and toe spreading were measured using ImageJ (NIH, Bethesda, MD, USA; Schneider et al., 2012), and the SFI was calculated using the formula from Bain et al. (1989). Results were averaged from 3 images to find a single SFI value for each rat at each time point.

Histology and imaging
Tissue was blocked in OCT (4583, TissueTek/Sakura Finetek USA, Torrance, CA, USA), and subsequently sectioned using a cryostat into 10 μm sections, sliced axially. Sections were collected approximately 5 mm proximal and 5 mm distal to the site of the injury. Slides were stored at –80°C until stained. Slides were washed in Millipore water and fixed in 10% formalin. Following fixation, slides were permeated using 0.2% Triton-X. Slides were then blocked in goat blocking buffer (10% goat serum (v/v) and 3% BSA (w/v) in PBS, and then incubated with the primary antibodies, mouse anti-β3-tubulin (Sigma-Aldrich, St. Louis, MO, USA; Cat# T5076, 1:500 dilution) and rabbit anti-laminin (Sigma-Aldrich; Cat# L9393, 1:500 dilution), for 1 hour at room temperature. Slides were then incubated with AlexaFluor 488 goat-anti-rabbit and AlexaFluor 594 goat-anti-mouse secondary antibodies (Life-Technologies; Cat# A-11008 and A-11005, respectively, 1:200 dilution) while being protected from direct light for 45 minutes at room temperature. Finally, slides were coverslipped with Vectashield (Vector Labs, Burlingame, CA, USA). Slides were then stored at 4°C and imaged within 1 week of staining.

Images were taken using a Leica SP-5 confocal microscope (Leica, Buffalo Grove, IL, USA) and 10×/0.4NA and 63×/1.3NA objectives, using filter sets appropriate for the above secondary antibodies. At 63×, images were taken confocally using z-stacks, from the bottom to the top of the sample. 63× images were taken randomly across the nerve section, covering approximately 50% of the nerve cross-sectional area, to representatively characterize the entire sample. Axons were counted using the z-projection of these 63× images by two individuals, using ImageJ; one member, blinded to the experiments, counted axons manually within each image. The other counted axons by image thresholding, using the "analyze particles" function in ImageJ, excluding very small particles (< 1 μm^2 in area). Total axon counts reflected summed counts from each image. Counts showed no significant difference when compared between lab member, with averaged counts within 5% of each other, and the final count used was an average between lab members. The average axon density was found by dividing the sum of axon counts by the sum of analyzed image areas. Non-nerve regions and large blood vessels, identified morphologically, were not included in area calculations. Total intra-epineurial area (*i.e.*, area of nerve within the inner epineurial border) was found by tracing the corresponding contour (ImageJ) in 10× images. Total axon counts were calculated by multiplying the average axon density by the inter-perineurial area. From the "analyze particles" function, average axon size (or the area stained at each point) was collected from each image. Fraction axon coverage was calculated as the total area within the nerve cross-section covered by axons divided by the total area of the image.

Statistical analysis
Significance for strain measurements and SFI was tested using a mixed two-way analysis of variance (ANOVA) (across: group, within: time), and Tukey's honestly significant difference (HSD) post hoc test was used to compare means between individual groups. Axon growth was tested using one-way ANOVA, comparing proximal and distal ends separately, again using Tukey's HSD post hoc test to compare means. All analysis was done in GraphPad Prism 7.04 (GraphPad Software, San Diego, CA, USA). Effect sizes were calculated using G*Power. For sample sizes used in our study, we were able to detect an effect size of 0.81 with a power of 0.80 (α = 0.05). Measurements are reported as the mean ± standard error of the mean (SEM).

Results
Integrity of varying nerve gaps repaired end to end
We first repaired rat sciatic nerve gaps of increasing length (corresponding to increasing tension) in terminal surgeries, and tested whether repairs could successfully tolerate joint movement corresponding to maximum nerve strain (knee extension and ankle dorsiflexion). All repairs were successfully completed in a neutral joint configuration. 1 and 2 mm gaps were successfully repaired with three epineurial sutures (*n* = 4 each), and did not fail following knee extension and ankle dorsiflexion. In contrast, though 3mm gaps were successfully

repaired with three epineurial sutures ($n = 4$), all (100% of) repairs showed signs of failure after knee extension and ankle dorsiflexion. Modes of failure included suture pullout, tearing of the epineurium surrounding the suture, or changes in nerve geometry in the vicinity of sutures. Even after reinforcing repairs with up to 7–8 epineurial sutures, repairs failed 25% of the time following joint manipulation (**Figure 2**).
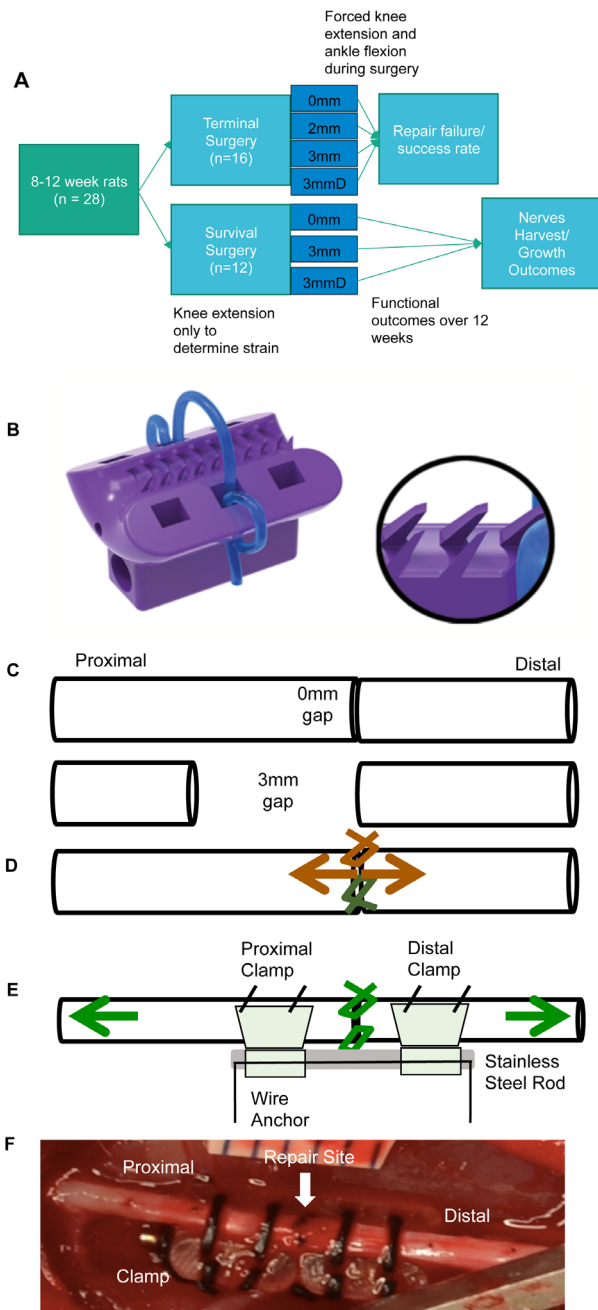

Figure 1 Summary of experimental design and implementation.
(A) Experimental flow and outcomes collected from terminal and survival surgery cohorts. (B) Design of the 3D printed clamp used in the device, with inset showing epineurial barbs. (C–E) Surgical procedure for survival surgeries and design of nerve device. (C) Initial injury of the sciatic nerve for 0 mm group (top) and 3 mm/3 mmD (nerve-interfacing device implantation) groups (bottom). (D) End-to-end repair of the sciatic nerve. (E) Device implantation for 3 mmD group and image of a completed implantation (F). Arrows in D and E show site and direction of tension.

Based on these qualitative assessments, we established 3 mm as the maximum allowable nerve gap amenable to end-to-end repair in our model, but whose repair is susceptible to damage in extreme physiological joint configurations. We then tested the feasibility of reinforcing the repair site with our NID. First, we tested whether the NID itself was likely to cause compressive damage to the nerve, by deploying it upon an uninjured nerve. Nerve conduction velocity was not significantly changed after deploying the NID on untransected nerves (31.28 ± 2.89 *vs*. 26.02 ± 4.72, $P > 0.36$), suggesting that the NID itself, as envisioned by its design, did not cause appreciable damage to neural elements (**Figure 3**). We then repaired 3 mm gaps in the presence of the NID. In contrast to repairs without the NID, all repairs were executed with the usual three sutures, and withstood knee extension and ankle dorsiflexion with no signs of repair failure or nerve damage. As an extreme example of NID functionality, we also repaired a 5-mm gap in the presence of an NID, with no signs of repair failure.

**Regenerative outcomes following end-to-end repair of varying gap size**
Based on the above observations in terminal surgeries, we performed survival surgeries to probe regenerative outcomes in three end-to-end repair groups: 0 mm gap (repair under
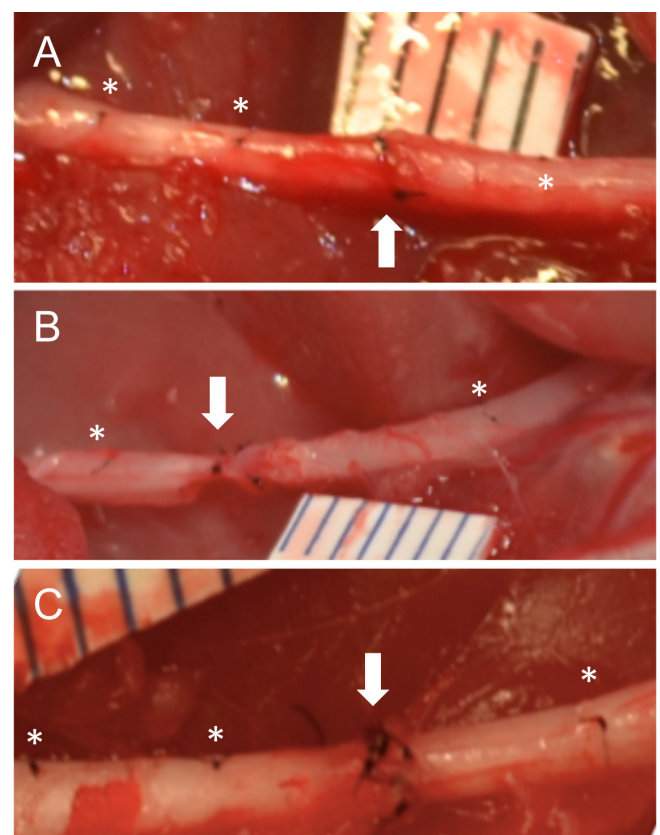

Figure 2 Successful and failed end-to-end repairs following sciatic nerve transection.
(A) Successful end-to-end repair. (B) Failed end-to-end repair. (C) Failed end-to-end repair that had been anchored with additional sutures. The repair site is indicated with arrows. Epineurial sutures used to measure changes in nerve length are indicated with asterisks.

minimal tension), 3 mm gap (repair under high tension), and 3 mm-NID group (repair under high tension, with tension redistributed away from repair site). For survival surgeries, based on the potential catastrophic repair failure of 3 mm gaps with combined knee and ankle movement, we ranged only the knee joint following repair, to confirm the integrity of repair. All repairs remained intact at the time of repair.

To probe local deformation following end-to-end repair in each group, we measured strain just proximal and just distal to the repair site. Immediately after repair, consistent with a larger gap, strain was significantly higher ($P = 0.0002$) in the distal region of the 3 mm gap group compared with the 0 mm gap. However, in the group with a device, this strain was partially relieved (**Figure 4B**). After 12 weeks, any differences in strain between groups were no longer significant (**Figure 4C**). In addition, after 12 weeks we observed significantly increased spacing between sutures with knee and ankle in a neutral configuration, indicative of material addition ("growth") between the sutures over 12 weeks (**Figure 5B**). Such growth in both 3 mm and 3 mm-NID groups appeared to exceed growth in the contralateral limb.
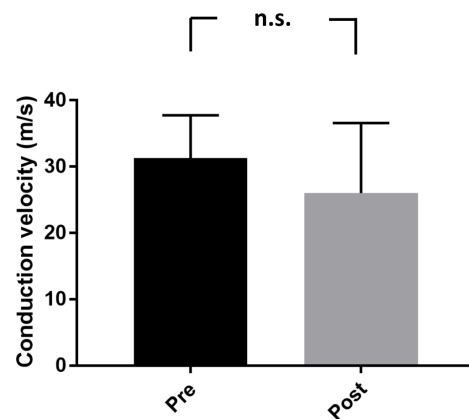
Figure 3 Conduction velocity pre- and post-device implementation on uninjured sciatic nerves.
No significant changes occurred in velocity before and after device implantation in uninjured nerves. Slight difference in conduction velocity average between groups is due to a single outlier. Bars represent standard error ($n = 10$). n.s.: Not significant.

*$P = 0.03$
***$P = 0.0002$
Row factor (Treatment): $P = 0.0008$
Column factor (location): $P = 0.003$
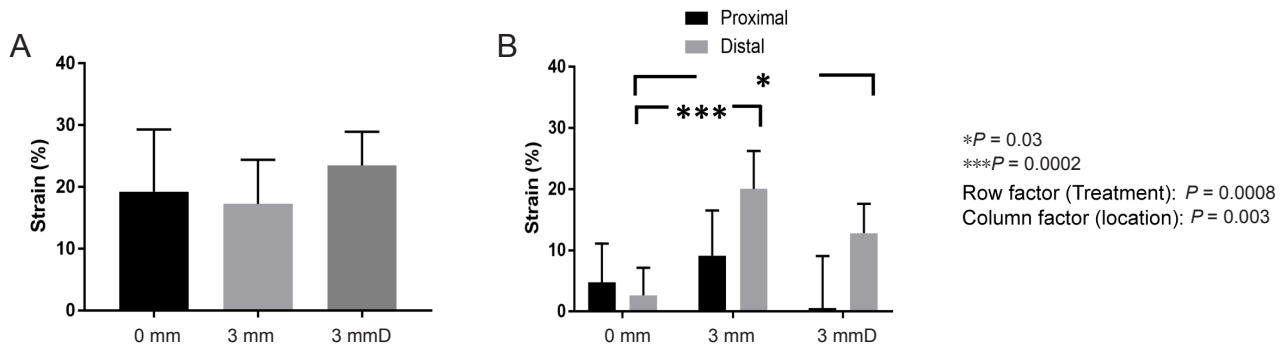
Figure 4 Strain in injured and uninjured sciatic nerves.
(A) Strain in the uninjured contralateral nerve with knee extension. (B) Strain that occurred with knee extension after nerve injury. (C) Strain that occurred with knee extension after 12 weeks recovery. 3 mmD: nerve-interfacing device implantation. Bars represent standard error ($n = 18$). *$P < 0.05$, ***$P < 0.001$ (two-way analysis of variance followed by Tukey's honestly significant difference (HSD) *post hoc* test).
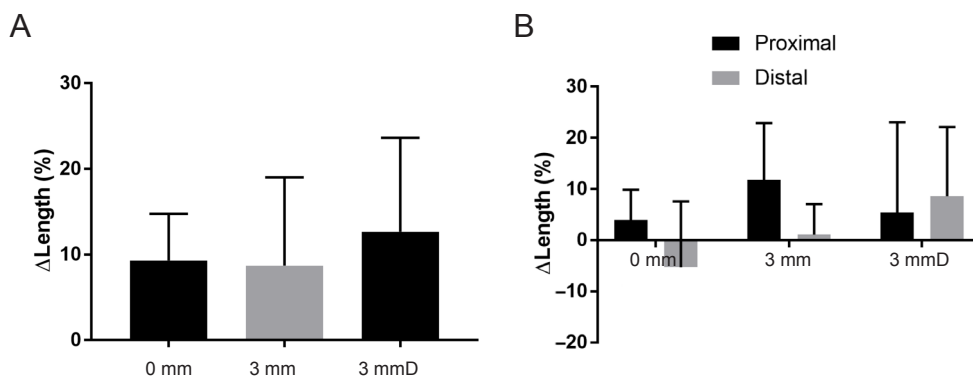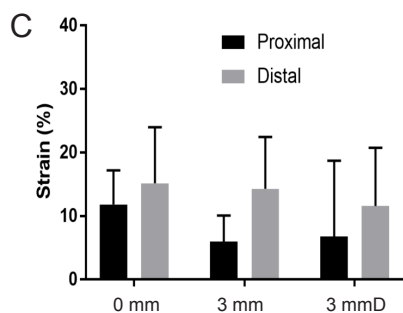
Figure 5 Nerve "growth" over 12 weeks after sciatic nerve injury and repair.
Growth was assessed based on distance between two sutures in the contralateral nerve (A) and the injured nerve (B). Bars represent standard error ($n = 18$). 3 mmD: Nerve-interfacing device implantation.

Functionally, SFI decreased after injury, consistent with the loss of sciatic nerve function (**Figure 6**). During recovery, ANOVA revealed a significant effect of time, but no difference in SFI across experimental groups, suggesting consistent, but incomplete recovery after 12 weeks in all groups. At 12 weeks, upon exposure of the nerve, repairs appeared intact in all groups. Enhanced fibrotic deposition was observed in device groups; however, devices were readily removed from the attached nerve prior to tissue harvest (**Figure 7**). Consistent with the similarity of functional outcomes across groups, axon growth also appeared similar among groups, with no significant differences in axon counts between groups (**Figures 8, 9A,** and **9B**). Interestingly, the axon size was significantly higher in the 3 mm (no device) group compared with the other groups, consistent with increased gross indicators of growth (**Figure 9C** and 9**D**).

Discussion

Redistribution of tension away from the repair site enabled end to end repair of larger gaps

In this study, we repaired nerves end-to-end under varying tension, with and without a new device that redistributed tension away from the site of repair. Repairs of large nerve gaps failed in physiological joint configurations resulting in maximum nerve strain. However, using a nerve-interfacing device we effectively redistributed tension at the repair site, and the novel clamp design held the nerves in place without damage. There was also no repair site failure when using the device, suggesting its potential utility in graft-free repairs, without detrimental effects. The device was also superior to simply adding additional epineurial sutures to the nerve to reinforce the repair, as loads could be distributed across the larger nerve-clamp interface, rather than at individual sutures. The strategy of redistributing tension away from the site of repair has been successfully tested surgically by Kechele et al. (2011), using a mesh, and Scherman et al. (2004), using anchoring sutures. Anecdotal evidence suggests that surgeons may also reinforce or protect repair sites by wrapping them with nerve conduits or other materials. In contrast, the use of a nerve interfacing device provides a simpler, more clinically reproducible and reliable approach. Advantages include the ability to readily align and approximate nerves to a desired strain during the repair, in a manner analogous to non-implantable tissue approximators used intra-operatively (Forootan et al., 2014). Gripping the nerve via epineurial barbs also represents a new approach to securing the nerve without excessive compression, while preserving conductive elements.

Cumulatively, our data suggested that the repairs made under tension were no worse than those made without tension. With respect to strain, functional, and histological outcomes, repairs under tension – with or without a device -- did not adversely affect nerve regeneration. The magnitudes of measured strains are consistent with previous studies in the rat sciatic nerve (Foran et al., 2017), and magnitudes of SFI and axon counts are consistent with several previous reports, which range from an average of 7000 to 12,000 axons distal to the repair (MacKinnon et al., 1991; Jonsson et al., 2013; Ganguly et al., 2017).

Our observed outcomes also reflect the key considerations that enter surgical decision-making. On one hand, repairs of the 3 mm device-free group failed catastrophically when nerves were maximally strained (knee extension and ankle dorsiflexion). However, no failures were seen with knee extension alone, or after 12 weeks with joint movement during recovery, and functional and structural outcomes trended more favorably compared to 0 or 3 mm-NID groups. We speculate that repair integrity may reflect the fact that after sciatic nerve injury, no active ankle dorsi- or plantar flexion can occur, thus protecting the nerve from any ankle-related tension. In addition, typical rat hindlimb postures do not maximally strain the sciatic nerve. Thus, if the repair holds, a tensioned repair of larger gaps is not unfavorable, and in fact, as demonstrated to be the case for smaller gaps, may even be favorable (Hentz et al., 1993; Sunderland et al, 2004). On the other hand, the fact that 3mm gaps repaired without a device fail in extreme, albeit still physiological, joint configurations demonstrates the high risk associated with tensioned repairs despite their possible benefit. Protection of the repair site, as we have shown with our NID, may offer the benefits of a tensioned repair while mitigating the risk. We recommend protection of the repair site over a timeframe during which the repair is structurally stabilized. Biomechanical properties of transected rat nerves significantly improve within seven days post-repair, and approach a plateau within 3 weeks post-repair, suggesting robust and rapid strengthening of the repair sites (Abrams et al., 1998); future versions of a resorbable device could reflect such timelines.

Role of tension in growth

An intriguing observation was that comparatively high (though not super-physiological) nerve strain observed immediately after repair in the 3 mm groups was markedly reduced after 12 weeks of recovery. Further, in the 3mm group, growth appeared to be, surprisingly, even more robust based on larger axon diameter and increased axon coverage. These findings support a hypothesis that tension may stimulate growth. There is considerable precedent for a positive role for nerve tension on growth. Previous studies have shown that the rate of axon growth increases when axons are under tension, even to the extent of multiplying the rate of growth by eight (Bray, 1984; Pfister et al., 2004). Other studies show that tension activates certain translational pathways, such as mTOR-based pathways, promoting further axon growth and structural changes (Suter and Miller, 2011; Love et al., 2017). Nerve lengthening also occurs in limb lengthening procedures, and if done slowly enough, without detriment to the affected nerves (Simpson et al., 2013). Similarly, decompressed nerves redistribute their strain to reflect their dynamic environment (Foran et al., 2018), suggesting a remarkable capacity for remodeling in response to mechanical cues. This concept has increasingly been incorporated into neuroregenerative strategies by multiple research
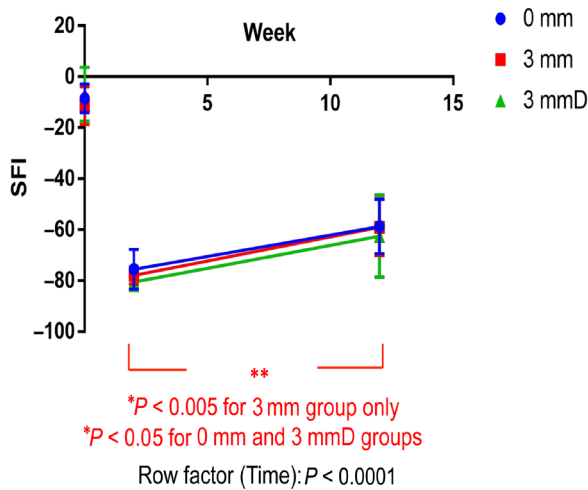
Figure 6 Change in SFI over time after sciatic nerve injury.
SFI improves significantly ($P < 0.0001$) 12 weeks after injury (two-way analysis of variance followed by Tukey's honestly significant difference (HSD) *post hoc* test). Bars represent standard error ($n = 18$). 3 mmD: Nerve-interfacing device implantation group. SFI: Sciatic functional index.
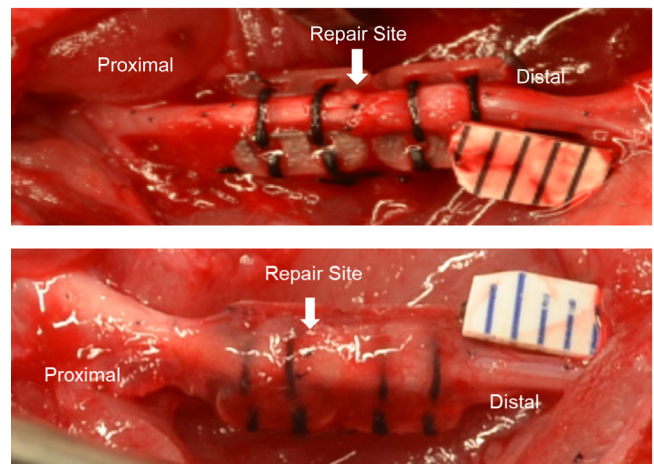
Figure 7 Injury appearance before and after recovery with device implantation
Nerve device immediately following implantation (top) and 12 weeks post implantation (bottom), showing a fibrotic layer that has formed over the clamps. Device was cleanly excised from the sciatic nerve upon removal of this layer.
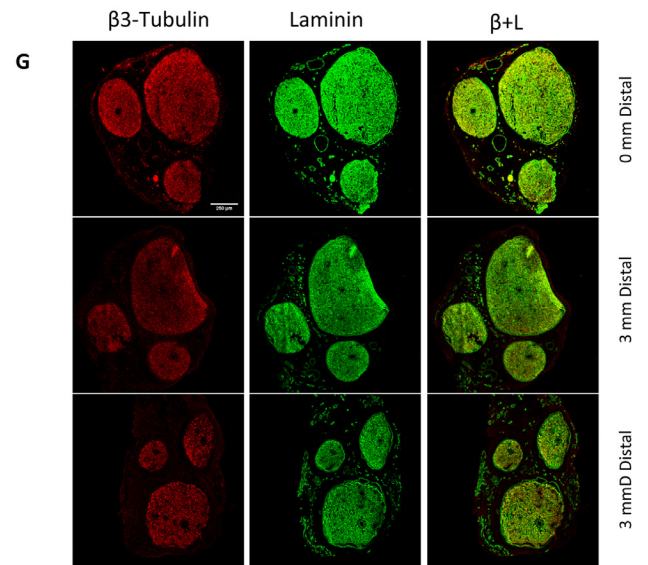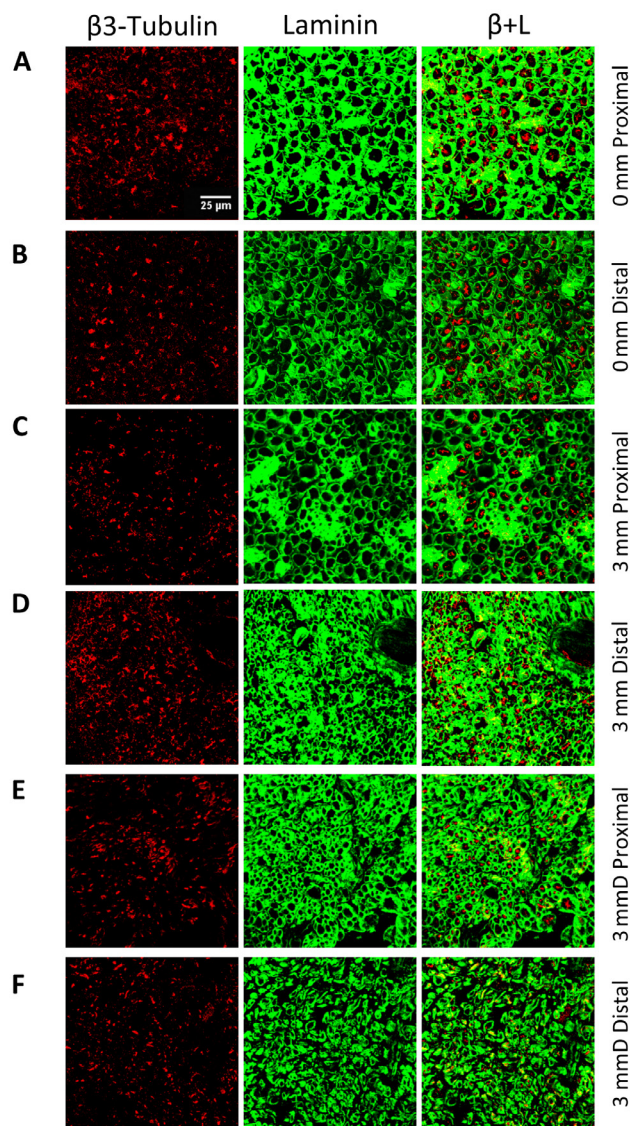
Figure 8 Staining with laminin and β3-tubulin antibodies of injured nerves 12 weeks after sciatic nerve repair.
0 mm group proximal (A) and distal (B) to the injury. 3 mm group proximal (C) and distal (D) to the injury. 3 mmD (nerve-interfacing device implantation) group proximal (E) and distal (F) to the injury. Blood vessels were excluded from the analysis, and all images are at the same scale. (G) 10× images of distal nerves from each group provide examples of images used to make total cross-sectional area measurements. Red is β3-tubulin, green is laminin.
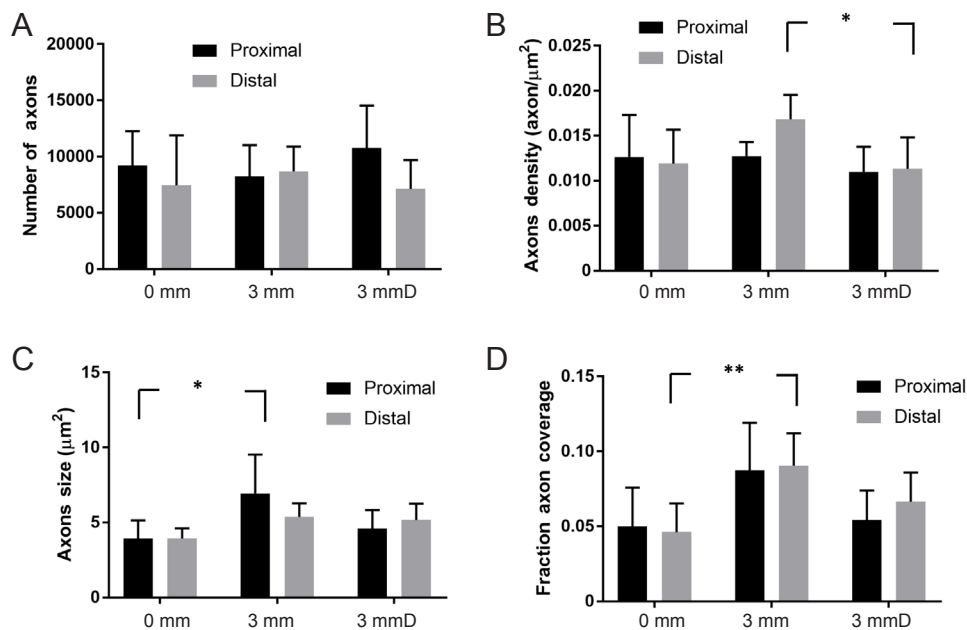
Figure 9 Quantitative analysis of confocal images at 12 weeks after sciatic nerve repair.
(A) Number of axons; (B) axon density, or the number of axons per area; (C) axon size; (D) fraction axon coverage, or the area covered by axons divided by the total area inside the perineurium. Significant differences were found using multiple comparison tests between 3 mm and 3 mmD (nerve-interfacing device implantation) axon density, distally ($*P < 0.05$); between 0 mm and 3 mm axon size, proximally ($*P < 0.05$), and between 0 and 3 mm axon coverage, distally ($**P < 0.01$) (one-way analysis of variance followed by Tukey's honestly significant difference (HSD) *post hoc* test). Bars in all graphs represent the standard error ($n = 17$).

groups, with positive results (Saijilafu et al., 2008; Chuang et al., 2013; Vaz et al., 2014; Yousef et al., 2015). Finally, a case report suggests that dynamic tensioning can have favorable outcomes as well (McDonald and Bell, 2010), providing early clinical support for tensioned repairs, under appropriate circumstances.

Limitations
Despite promising data in support of tensioned repairs, our study did have several limitations. First, because tissue was sampled at a single time point and location, it was not possible to determine how axon growth rate was ultimately affected by tension. However, we were able to determine that functional recovery and axon growth distal to the injury occurred, revealing that the repairs under tension were, at minimum, as effective as tension-free repairs. Further study, by allowing longer recovery times and sampling structural regeneration at additional intermediate data points, could reveal the effect of tension on axon growth with increased resolution. Another limitation was our small sample sizes, compared to other studies. However, power analysis suggests that we were able to detect effect sizes of 0.81 with a power of 0.80, and based on our data, establishing significant differences between groups would require at minimum 2–3× the sample size in these experiments. Thus our study is sufficiently powered to confirm a lack of major differences from group to group. A third limitation was our decision to use strain as a surrogate for tension, not measure tension itself. This was in part due to significant nerve-to-nerve differences in material properties, and in part due to the ability to readily measure regional differences in deformation. Another limitation was our selected approach for functional testing. We had two goals; the first was to measure conduction velocity in uninjured nerves, to demonstrate device implantation did not appreciably affect neural elements. This was achieved using electromyography-based conduction

testing. Our second goal was to use simple functional outcomes to demonstrate that device implantation and repairs under tension did not adversely affect functional regeneration (*i.e.*, that such approaches are safe). Towards this goal, we elected to use the SFI, a measure that is not considered as reliable for earlier time points, but shows good correlation with recovery at later time points, and so remains a simple and useful tool for longitudinally measuring recovery (Monte-Raso et al., 2008). Future studies would benefit from the use of additional functional tests, including conduction velocity testing, muscle contractility, and/or joint torque testing. Finally, with respect to translation of our NID, while Visijet M3 Crystal is USP Class VI approved, this material is non-resorbable, and thus an additional surgery would be required for device excision. However, the use of resorbable materials (*e.g.*, PLGA), which are widely used in a variety of biomedical devices, offer a solution to this translational challenge.

Conclusions and clinical implications
Currently, clinicians are rightfully reluctant to make nerve repairs under tension. However, this study as well as other previous literature suggests that tension could be a valuable alternative to the use of grafts in cases of small to moderately sized nerve gaps. With the caveat that the repair is stable – a concern addressed by our novel NID – tension is not detrimental to the repair and may even promote faster growth. This concept may be pushed further in future research, in which dynamic tensioning *via* modified versions of the NID may be used to bridge much larger nerve gaps prior to performing end-to-end repairs (Vaz et al., 2014).

References

Abrams RA, Butler JM, Bodine-Fowler S, Botte MJ (1998) Tensile properties of the neurorrhaphy site in the rat sciatic nerve. J Hand Surg Am 23:465-470.

Bain JR, Mackinnon SE, Hunter DA (1989) Functional-evaluation of complete sciatic, peroneal, and posterior tibial nerve lesions in the rat. Plast Reconstr Surg 83:129-136.

Bhatia A, Doshi P, Koul A, Shah V, Brown JM, Salama M (2017) Contralateral C-7 transfer: is direct repair really superior to grafting? Neurosurg Focus 43:E3.

Bray D (1984) Axonal growth in response to experimentally applied mechanical tension. Dev Biol 102:379-389.

Bustamante J, Socolovsky M, Martins RS, Emmerich J, Pennini MG, Lausada N, Domitrovic L (2011) Effects of eliminating tension by means of epineural stitches A comparative electrophysiological and histomorphometrical study using different suture techniques in an animal model. Arq Neuropsiquiatr 69:365-370.

Chuang TH, Wilson RE, Love JM, Fisher JP, Shah SB (2013) A novel internal fixator device for peripheral nerve regeneration. Tissue Eng Part C Methods 19:427-437.

Forootan K, Karimi H, Forootan NS (2014). A new device for nerve approximation in traumatic injuries of extremities. Eur J Plast Surg 37:497-502.

Franze K, Guck J (2010) The biophysics of neuronal growth. Rep Prog Phys 73:4601-4619

Ganguly A, McEwen C, Troy EL, Colburn RW, Caggiano AO, Schallert TJ, Parry TJ (2017) Recovery of sensorimotor function following sciatic nerve injury across multiple rat strains. J Neurosci Methods 275:25-32.

Grinsell D, Keating CP (2014) Peripheral nerve reconstruction after injury: a review of clinical and experimental therapies. Biomed Res Int 2014:698256.

Guneren E, Odaci E, Yildiz L, Akbas H, Eroglu L, Kaplan S (2004) Use of longitudinal invaginating matrix sutures in microarterial sleeve anastomoses. Scand J Plast Reconstr Surg Hand Surg 38:1-4.

Hentz VR, Rosen JM, Xiao SJ, McGill KC, Abraham G (1993) The nerve gap dilemma: a comparison of nerves repaired end to end under tension with nerve grafts in a primate model. J Hand Surg Am 18:417-425.

Jonsson S, Wiberg R, McGrath AM, Novikov LN, Wiberg M, Novikova LN, Kingham PJ (2013) Effect of delayed peripheral nerve repair on nerve regeneration, schwann cell function and target muscle recovery. PLoS One 8:e56484.

Kechele PR, Bertelli JA, Dalmarco EM, Frode TS (2011) The mesh repair: tension free alternative on dealing with nerve gaps-experimental results. Microsurgery 31:551-558.

Love JM, Bober BG, Orozco E, White AT, Bremner SN, Lovering RM, Schenk S, Shah SB (2017) mTOR regulates peripheral nerve response to tensile strain. J Neurophysiol 117:2075-2084.

Mackinnon SE, Dellon AL, O'Brien JP (1991) Changes in nerve fiber numbers distal to a nerve repair in the rat sciatic nerve model. Muscle Nerve 14:1116-1122.

Maeda T, Hori S, Sasaki S, Maruo S (1999) Effects of tension at the site of coaptation on recovery of sciatic nerve function after neurorrhaphy: Evaluation by walking-track measurement, electrophysiology, histomorphometry, and electron probe X-ray microanalysis. Microsurgery 19:200-207.

Mahan MA, Vaz KM, Weingarten D, Brown JM, Shah SB (2015) Altered ulnar nerve kinematic behavior in a cadaver model of entrapment. Neurosurgery 76:747-755.

Matsuyama T, Mackay M, Midha R (2000) Peripheral nerve repair and grafting techniques: a review. Neurol Med Chir (Tokyo) 40:187-199.

McDonald DS, Bell MS (2010) Peripheral nerve gap repair facilitated by a dynamic tension device. Can J Plast Surg 18:e17-19.

Meek MF, Coert JH, Robinson PH (2005) Poor results after nerve grafting in the upper extremity: Quo vadis? Microsurgery 25:396-402.

Monte-Raso VV, Barbieri CH, Mazzer N, Yamasita AC, Barbieri G (2008) Is the Sciatic Functional Index always reliable and reproducible? J Neurosci Methods 170:255-261.

Pfister BJ, Iwata A, Meaney DF, Smith DH (2004) Extreme stretch growth of integrated axons. J Neurosci 24:7978-7983.

Pfister BJ, Gordon T, Loverde JR, Kochar AS, Mackinnon SE, Cullen DK (2011) Biomedical engineering strategies for peripheral nerve repair: surgical applications, state of the art, and future challenges. Crit Rev Biomed Eng 39:81-124.

Restaino SM, Abliz E, Wachrathit K, Krauthamer V, Shah SB (2014) Biomechanical and functional variation in rat sciatic nerve following cuff electrode implantation. J Neuroeng Rehabil 11:73.

Saijilafu, Nishiura Y, Hara Y, Yoshii Y, Ochiai N (2008) Simultaneous gradual lengthening of both proximal and distal nerve stumps for repair of peripheral nerve defect in rats. Muscle Nerve 38:1474-1480.

Scherman P, Kanje M, Dahlin LB (2004) Bridging short nerve defects by direct repair under tension, nerve grafts or longitudinal sutures. Restor Neurol Neurosci 22:65-72.

Schmidt CE, Leach JB (2003) Neural tissue engineering: Strategies for repair and regeneration. Annu Rev Biomed Eng 5:293-347.

Schneider CA, Rasband WS, Eliceiri KW (2012) NIH Image to ImageJ: 25 years of image analysis. Nat Methods 9:671-675.

Siemionow M, Sonmez E (2010) Peripheral Nerve Injuries. In: Plastic and Reconstructive Surgery (Siemionow MZ, Eisenmann-Klein M, eds). London: Springer London.

Simpson AH, Gillingwater TH, Anderson H, Cottrell D, Sherman DL, Ribchester RR, Brophy PJ (2013) Effect of limb lengthening on internodal length and conduction velocity of peripheral nerve. J Neurosci 33:4536-4539.

Sunderland IRP, Brenner MJ, Singham J, Rickman SR, Hunter DA, Mackinnon SE (2004) Effect of tension on nerve regeneration in rat sciatic nerve transection model. Ann Plast Surg 53:382-387.

Suter DM, Miller KE (2011) The emerging role of forces in axonal elongation. Prog Neurobiol 94:91-101.

Terzis J, Faibisoff B, Williams HB (1975) The nerve gap: suture under tension vs. graft. Plast Reconstr Surg 56:166-170.

Vaz KM, Brown JM, Shah SB (2014) Peripheral nerve lengthening as a regenerative strategy. Neural Regen Res 9:1498-1501.

Westerga J, Gramsbergen A (1993) Changes in the electromyogram of two major hindlimb muscles during locomotor development in the rat. Exp Brain Res 92:479-488.

Yousef MA, Dionigi P, Marconi S, Calligaro A, Cornaglia AI, Alfonsi E, Auricchio F (2015) Successful reconstruction of nerve defects using distraction neurogenesis with a new experimental device. Basic Clin Neurosci 6:253-264.